Received: 6 March 2018 | Revised: 30 March 2019 | Accepted: 5 July 2019

DOI: 10.4218/etrij.2018-0118

ORIGINAL ARTICLE

ETRI Journal WILEY

Automated epileptic seizure waveform detection method based on the feature of the mean slope of wavelet coefficient counts using a hidden Markov model and EEG signals

Miran Lee[1] | **Jaehwan Ryu**[2] | **Deok-Hwan Kim**[3]

[1]Graduate School of Information Science and Engineering, Ritsumeikan University, Shiga, Japan

[2]Technical Research Institute, Sammi Information System, Seoul, Rep. of Korea

[3]Department of Electronic Engineering, Inha University, Incheon, Rep. of Korea

Correspondence
Deok-Hwan Kim, Department of Electronic Engineering, Inha University, Incheon, Rep. of Korea.
Email: deokhwan@inha.ac.kr

Funding information
This research was supported in part by the Basic Science Research Program through the National Research Foundation of Korea funded by the Ministry of Education (2018R1D1A1B07042602) and in part by the Industrial Technology Innovation Program funded by the Ministry of Trade, Industry & Energy (MI, Korea) [10073154, Development of human-friendly human-robot interaction technologies using human internal emotional states] and in part by the Institute for Information & communications Technology Promotion(IITP) grant funded by the Korea government(MSIT) (No.2019-0-00064, Intelligent Mobile Edge Cloud Solution for Connected Car).

Long-term electroencephalography (EEG) monitoring is time-consuming, and requires experts to interpret EEG signals to detect seizures in patients. In this paper, we propose a novel automated method called adaptive slope of wavelet coefficient counts over various thresholds (ASCOT) to classify patient episodes as seizure waveforms. ASCOT involves extracting the feature matrix by calculating the mean slope of wavelet coefficient counts over various thresholds in each frequency subband. We validated our method using our own database and a public database to avoid overtuning. The experimental results show that the proposed method achieved a reliable and promising accuracy in both our own database (98.93%) and the public database (99.78%). Finally, we evaluated the performance of the method considering various window sizes. In conclusion, the proposed method achieved a reliable seizure detection performance with a short-term window size. Therefore, our method can be utilized to interpret long-term EEG results and detect momentary seizure waveforms in diagnostic systems.

KEYWORDS
discrete wavelet transform, electroencephalography, feature extraction, machine learning, Seizure detection

1 | INTRODUCTION

An epileptic seizure is a neurological episode that occurs when several nerve cells in the brain generate excessive and repetitive electric impulses over a short period of time, and approximately 1% to 2% of the global population suffers from epilepsy [1,2]. The diagnosis of epilepsy requires a long-term monitoring system, because information is required regarding the changes in biosignals obtained from patients in daily life. One widely employed method analyzes brain activity using electroencephalogram (EEG) signals [3]. However, analyzing seizures using continuous EEG (over 24 hours) not only takes a long time, but also requires experienced epileptologists. Therefore, an automatic

computer-based detection algorithm would be valuable for seizure detection using EEG.

Automatic computer-based methods for seizure detection have been utilized since the early 1970s [4]. Traditionally, a number of methods based on principal component analysis (PCA) [5–8] have been used, such as the wavelet transform-based method [9–13], key points based on local binary patterns [14], empirical mode decomposition [15–20], and zero-crossing [21–24]. Among these, wavelet transform (WT) can be utilized in seizure detection to accurately discriminate features from subbands to use for seizure classification [22]. Furthermore, as EEG signals are non-stationary, they are suitable for use in time–frequency domain methods, such as WT [12]. The decomposition of EEG records using WT provides both time and frequency contexts simultaneously, which makes it possible to accurately capture and localize transient features [25].

There have been several attempts to utilize WT for feature extraction in seizure waveforms. Kumar et al [9] proposed a scheme based on a discrete wavelet transform (DWT) analysis and the approximate entropy using an artificial neural network. Sharma et al [10] proposed a new approach based on the analytic time–frequency flexible wavelet transform and fractal dimension, and Bhati et al [11] designed a localized time–frequency three-band biorthogonal linear phase wavelet filter bank. Furthermore, Ocak [12] proposed a new scheme based on the approximate entropy and a discrete wavelet transform analysis. In addition, Nasehi et al [13] proposed a method based on wavelet transform features—such as the number of zero coefficients, largest coefficient, smallest coefficient, mean of coefficients, and standard deviation—of each subband, and a kernel Fisher discriminant analysis classifier. Satisfactory performances have been achieved using such WT-based methods. However, there are some challenges involved in using WT-based methods that should be addressed. One challenge is the diversity of seizure waveforms for the same patient, and another is that a large amount of training data is required for the training, which represents a burden for patients in a real-time application process [22].

Keeping in mind the aforementioned issues and motivation, we propose a computer-based classification method to classify episodes as seizures using a novel feature extraction algorithm utilizing discrete wavelet transform coefficients. The proposed method extracts the feature matrix by calculating the mean slope of wavelet coefficients counts over various thresholds in each frequency subband. To develop a robust and reliable seizure detection method, we utilized our own database as well as a public database. The proposed method was validated using our own database, and further tested with the public database to evaluate the generalizability and reliability.

A preliminary version of this work has been reported [26]; however, this paper provides additional quantitative results and proposes an improved and more sophisticated method for seizure detection, compared to that of the previous work.

The remainder of this paper is organized as follows. Section 2 describes the utilized databases. Section 3 presents the proposed seizure detection method. Next, the performance of the proposed method is demonstrated using two seizure databases in Section 4. Subsequently, Section 5 discusses the outcomes of experiments, and finally Section 6 concludes the paper.

2 | DATABASES

2.1 | Our database

For the development and verification of the proposed method for epileptic seizure waveforms, we acquired EEG signals from four healthy subjects and four patients who received a diagnosis of epilepsy from a medical doctor. It took approximately 33 minutes for EEG monitoring for each individual in this experiment. As shown in Figure 1, the offline experiments were conducted according to the international 10–20 system. In line with the international 10–20 system standards, all 19 channels (FP1, FP2, F3, F4, F7, F8, T3, T4, T5, T6, O1, O2, P3, P4, C3, C4, FZ, CZ, and PZ) and both ear lobes were used as the positions of the EEG electrodes to record the EEG signals [27]. Also, both electrooculography (EOG) and electrocardiography (ECG) signals were measured. EOG was used to observe the patient's eye movements when seizures occurred and ECG was measured for analyzing the variation and detecting subject's movement when seizures occurred because ECG signals contain real-world noise [28]. F, C, O, P, and T denote the frontal, central, occipital, parietal, and temporal lobes, respectively. The two ear lobes were utilized as the ground. We obtained clinical information, such as the time and channel of seizure occurrence, for all patients from medical doctors in advance. The sampling rate for the acquisition of EEG signals was set to 200 Hz per second, and this was sufficient to capture all signals to detect seizure EEG signals. An EEG dataset was acquired from Inha University Hospital with approval from the Institutional Review Board (IRB). Based on this database (we refer to this database as IHDB), we created nonseizure subsets (IHDB-N) from healthy subjects and seizure subsets (IHDB-S) from patients. We consider the following a class with subsets IHDB-N vs IHDB-S (IHDB-N-S).

2.2 | Public database

To validate our method, we utilized a public database of EEG signals provided by the University of Bonn, Germany [29]. We refer to this database as BNDB. This database contains EEG signals acquired from healthy subjects and patients. The database comprises five subsets (denoted as BNDB-Z, BNDB-O, BNDB-N, BNDB-F, and BNDB-S). The subsets BNDB-Z (eyes open) and BNDB-O (eyes closed) include EEG signals

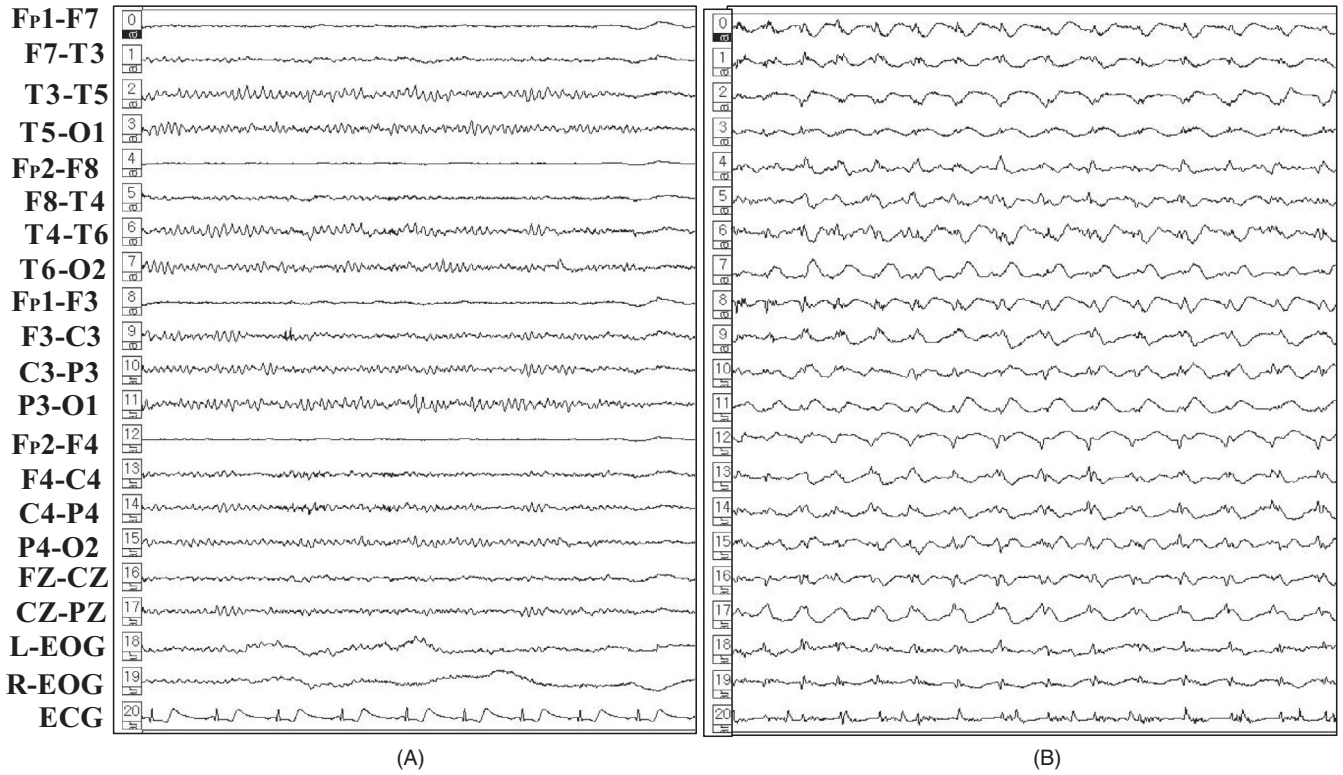

FIGURE 1 EEG signals from IHDB. (A) EEG record for normal adult; (B) EEG of seizure patient. (Indicators listed in the left column represent the electrode locations of the EEG. F: frontal; T: temporal; O: occipital; C: central; P: parietal; L-EOG: left-electrooculography; R-EOG: right-electrooculography; ECG: electrocardiography.)

recorded from five healthy subjects with their eyes open and closed, respectively. The subsets BNDB-N (epileptogenic zone) and BNDB-F (hippocampal formation) contain EEG signals recorded intracranially from epileptic patients during seizure-free intervals. The subset S contains EEG signals recorded from epileptic patients during seizure activity. In this study, we considered the following seven classes: subset BNDB-Z vs BNDB-S (BNDB-Z-S), subset BNDB-O vs BNDB-S (BNDB-O-S), subset BNDB-N vs BNDB-S (BNDB-N-S), subset BNDB-F vs BNDB-S (BNDB-F-S), subset BNDB-ZO vs BNDB-S (BNDB-ZO-S), subset BNDB-NF vs BNDB-S (BNDB-NF-S), and subset BNDB-ZONF vs BNDB-S (BNDB-ZONF-S). These classes were separated according to the seizure database.

3 | METHOD

We propose a wavelet-based approach to extract features from epileptic EEG signals. Figure 2 illustrates the general structure of the proposed method: adaptive slope of wavelet coefficient counts over various thresholds (ASCOT). This is a method for counting the number of times a given signal exceeds a certain threshold, repeating the steps while changing the threshold, and calculating the rate of change of the counted values. The detailed methodologies for each step will be described in the following subsections.

3.1 | Proposed wavelet-based approach

To decompose the frequency bands of EEG signals, we employed the DWT. It is useful to perform a multiresolution analysis on recorded EEG signals, because this can alleviate the disadvantage of the fixed time–frequency resolution of the short-time Fourier transform [30]. The DWT creates signals of different resolutions and frequency bands by decomposing raw signals into approximate and detailed information. A wavelet dictionary was designed using a zero-averaged basis function ψ, dilated using (1):

$$\int_{-\infty}^{\infty} \psi(t)\,dt = 0,$$

$$\psi_{a,b}(t) = \frac{1}{\sqrt{a}} \cdot \psi\left(\frac{t-b}{a}\right), \tag{1}$$

where a is a scale factor and b is a translation factor. The DWT was determined by using discrete parameters for any scale a_0 and position b_0 ($a_0 \geq 1$, $b_0 \geq 1$) with (2):

$$\mathrm{DWT}(a,b) = \frac{1}{\sqrt{a_0^i}} \int_{-\infty}^{\infty} x(t) \cdot \psi^*\left(\frac{t - kb_0a_0^i}{a_0^i}\right) dt, \tag{2}$$

where k and i are integers, and $a^{-1/2}$ is the constant of energy normalization.

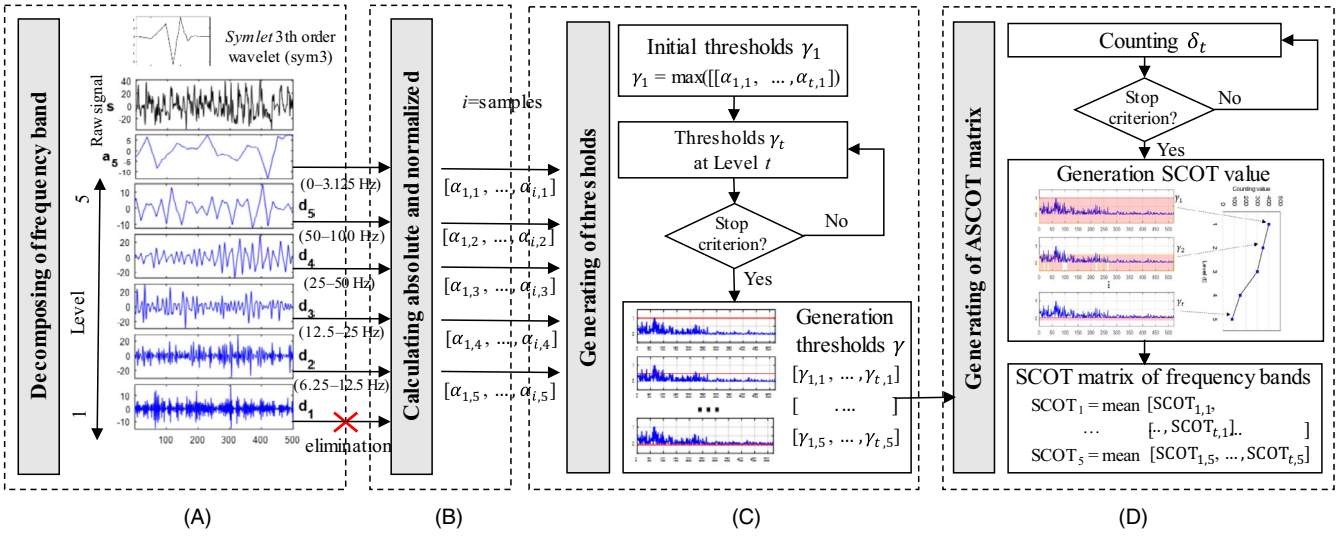

FIGURE 2 General structure of the proposed ASCOT method: (A) decomposition of frequency bands; (B) calculation of absolute and normalized coefficients; (C) generation of thresholds; and (D) generation of ASCOT matrix

Choosing an appropriate wavelet and number of levels of decomposition is important in the analysis of EEG signals using the DWT [30]. Figure 3 depicts various wavelet functions, such as *Symlete* (abbreviated as Sym), *Daubechies* (Db), and the *Coiflet* (Coi) mother wavelet function. The decomposition is performed using the mother wavelet that is most similar to the epileptic seizure signal waveform. In this study, we used a Sym wavelet to decompose the frequency bands of EEG signals, because this employs a sharper wavelet function, which closely reflects the continuous EEG signal's characteristics. We implemented the cross-correlations between an epileptic seizure signal waveform and various wavelet functions (Sym, Db, and Coi). Figure 4 illustrates the performances of the normalized means of the cross-correlations between various wavelet functions and the epilepsy waveform. Among these, Sym of order 3 obtains the highest mean of correlation coefficients with epilepsy waveforms. Therefore, we chose the Sym of order 3 wavelet in this study.

The EEG signal was decomposed into five decomposition levels, with detail coefficients D1–D5 and approximation

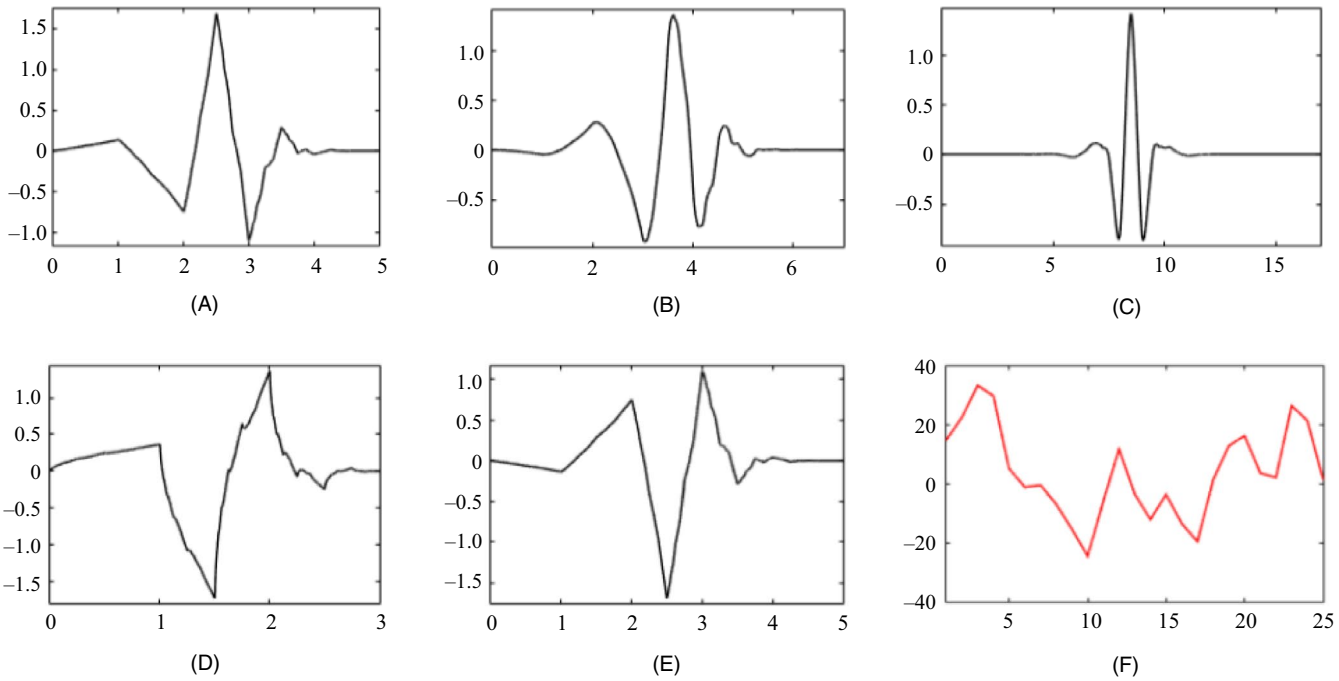

FIGURE 3 Comparison of mother wavelet functions and epileptic seizure waveform; (A–E) wavelet function; (A) Daubechies of order 3; (B) Daubechies of order 4; (C) Coiflet of order 3; (D) Symlet of order 3; (E) Symlet of order 4; and (F) shape of an epileptic seizure waveform

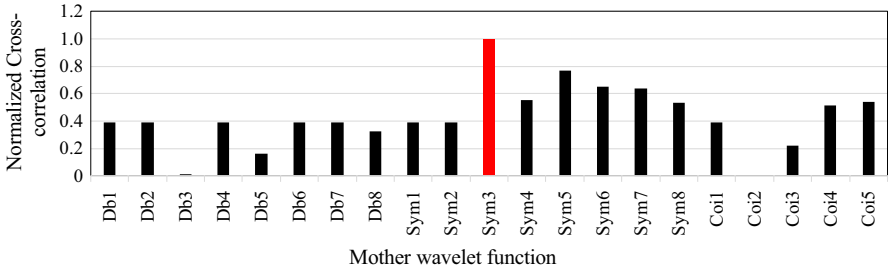

FIGURE 4 Cross-correlation between various wavelet functions and the epileptic seizure waveform. The x-axis shows wavelet functions and the y-axis represents the mean of the cross-correlation of each wavelet function

coefficients A1–A5. Here, D and A denote the detail and approximate coefficients, respectively. The index number with a dash (–) indicates the decomposition level. As the sampling rate is set as 200 Hz, the categories of decomposed EEG signals are D1 (50 Hz–100 Hz), D2 (25 Hz–50 Hz), D3 (12.5 Hz–25 Hz), D4 (6.25 Hz–12.5 Hz), D5 (3.125 Hz–6.25 Hz), and A5 (0 Hz–3.125 Hz). EEG signals do not have useful frequency components above 30 Hz, and the descriptor information of the seizure waveform is contained in decomposition levels 2 to 5 [27]. Hence, we focused on the subband details of D2 to D5 (frequency range 6.25 Hz–25 Hz) and the approximation A5 (frequency range 0 Hz–25 Hz) to extract the feature vectors.

3.2 | Feature extraction

We generated features for seizure waveforms based on the coefficients of each subband extracted using the DWT. This approach was based on the advantage of the zero-crossing method [31] for measuring the frequency or the period of a periodic signal. As shown in Figure 2D, in the step of generating the ASCOT matrix, $\delta(t)$ is a counting value, obtained by counting the normalized-absolute wavelet coefficient α values over a specified threshold γ_t in a specific level t, as expressed in (3):

$$\delta(t) = \sum_{i=1}^{N} f\left[\alpha_k\right],$$

$$f\left[\alpha_k\right] = \begin{cases} 1, & \alpha_k \geq \gamma_t \\ 0, & \text{otherwise} \end{cases}. \tag{3}$$

The threshold γ_t at level t represents a specified threshold corresponding to each level. Figure 2C illustrates the step of finding the threshold. An initial threshold γ_1 is calculated as the product of the inverse m-value and the maximum value among the normalized-absolute wavelet coefficients $\{\alpha_1, \alpha_2, \ldots, \alpha_N\}$ in each frequency subband. Other thresholds are obtained using (4):

$$\gamma(t) = \gamma_1 \cdot \left(\frac{1}{m}\right)^{t-1} \quad t \geq 2. \tag{4}$$

We repeat the applications of (3) and (4) until the threshold values of all levels are obtained. The threshold level t proceeds until there is no further change in the counting value δ in each step. The m-values are used to determine the threshold, and the range of m-values is 2 to 10. The experimental results show that almost all m-values in the range from 2 to 9 result in a high accuracy, and the highest accuracy is obtained when the m-value is 2. Therefore, we set m as 2 in all experiments. Finally, the difference values between the δ value at level $t+1$ and the previous δ value at level t are obtained, and the mean of these difference values is calculated as the ASCOT value using (5):

$$\text{ASCOT} = \frac{1}{t}\sum_{i=1}^{t-1}\left(\delta_{i+1} - \delta_i\right)^2. \tag{5}$$

This step is required to obtain the distribution of the seizure waveforms, which may vary according to the recorded signal or an individual's characteristics, by using the rate of change of the counted values according to levels. Further, by repeatedly measuring the frequency change and using the ratio of the counting values, it is possible to further reflect the inherent characteristics of seizure waveforms.

3.3 | Classification

Figure 5 illustrates our proposed hidden Markov model (HMM). A HMM can be represented as a sequential process. This is based on a chain model, in which future and current states are determined by the previous state [32]. In this study, we generated two training HMMs, which are defined as $\lambda = \{\mathbf{A}, \mathbf{B}, \pi\}$, where $\mathbf{A}$ is a state transition probability matrix. Each a_{ij} represents the probability of moving from state i to state j, $\mathbf{B}$ represents the observation symbol probability matrix, b_j is the emission probability, O is the observation, and π is the initial state probability. Finally, we can employ the observation symbol sequence O to select the model with the highest likelihood among all trained seizure and nonseizure HMMs.

4 | RESULTS

To validate the proposed ASCOT with the HMM method, various classification methods were considered to classify the seizure classes, including support vector machine (SVM)

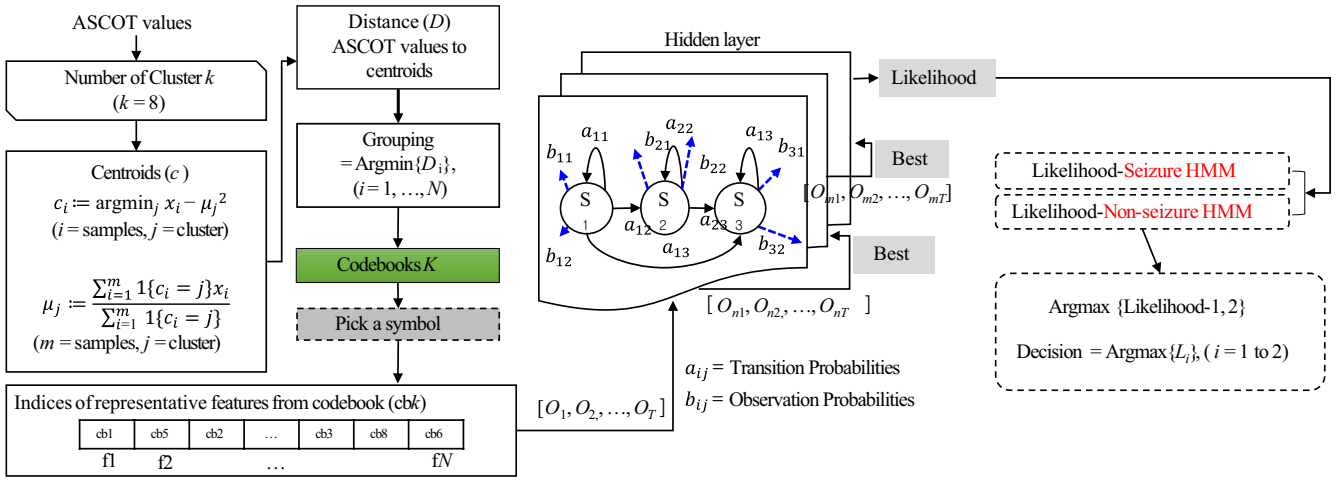

FIGURE 5 General structures of seizure and nonseizure HMMs

(linear, polynomial, and radial basis function (RBF) kernel functions), linear discriminant analysis (LDA), quadratic discriminant analysis (QDA), *k*-nearest neighbor (*k*-NN), multilayer perceptron neural network with the back propagation training algorithm (MLPNN with BP), and C4.5 decision tree (DT).

4.1 | Performance measures

To measure classification performance, the sensitivity (SEN = TP/(TP + FN)), specificity (SPE = TN/(TN + FP)), and accuracy (ACC = (TP + TN)/(TP + TN +FP + FN)) are calculated using the true positives (TP), false positives (FP), true negatives (TN), and false negatives (FN) [28]. TP is the number of positives identified by both the detection method and experts. FP is the number of positives identified by experts but missed by the detection method. Conversely, TN is the number of negatives identified by the detection method and by experts, and FN is the number of negatives identified by experts but missed by the detection method [33].

4.2 | Performance evaluation using various classifiers based on IHDB and BNDB

We verified our algorithm using Sym of order 3, which had the highest correlation with seizure waveforms based on the two databases BNDB and IHDB (Table 1). For the public database BNDB, the accuracy of proposed method with HMM was 99.78%, which was the highest performance. For our own database IHDB, the proposed method using LDA yielded the worst accuracy of 91.29%, whereas that using the HMM classifier yielded a high accuracy of 98.93%. With the

TABLE 1 Performance comparison of the proposed method with Sym 3 using various classifiers based on BNDB and IHDB

	BNDB			IHDB		
Classifier	**SEN (%)**	**SPE (%)**	**ACC (%)**	**SEN (%)**	**SPE (%)**	**ACC (%)**
SVM (linear)	98.54 (1.56)	98.65 (3.35)	98.51 (1.78)	94.80 (1.41)	96.12 (0.74)	96.73 (0.71)
SVM (polynomial)	99.12 (1.23)	99.51 (0.51)	99.77 (0.55)	96.12 (1.09)	97.32 (0.30)	96.72 (0.23)
SVM (RBF)	98.79 (1.06)	98.52 (0.54)	99.01 (0.23)	97.07 (0.74)	96.31 (3.13)	98.41 (0.75)
LDA	95.56 (2.77)	91.56 (4.46)	93.22 (4.05)	91.84 (1.06)	92.74 (1.15)	91.29 (0.30)
QDA	95.34 (1.98)	92.85 (3.87)	94.56 (2.53)	93.39 (1.24)	93.49 (0.57)	94.25 (1.48)
k-NN	94.55 (2.42)	96.78 (2.70)	95.55 (3.35)	96.34 (0.33)	96.14 (0.79)	94.99 (0.58)
MLPNN with BP	98.88 (1.52)	98.67 (0.21)	98.12 (0.37)	93.61 (3.14)	98.55 (0.20)	97.09 (0.30)
DT (C4.5)	99.08 (0.91)	99.33 (0.21)	99.53 (1.09)	98.13 (2.25)	96.79 (1.38)	98.13 (1.21)
HMM	**99.73 (0.43)**	**99.53 (0.60)**	**99.78 (0.40)**	**96.54 (0.05)**	**98.75 (0.49)**	**98.93 (0.68)**

Bold values indicate the highest performance among various classifiers.

Abbreviations: ACC, accuracy; DT, decision tree; HMM, hidden Markov model; *k*-NN, *k*-nearest neighbor; LDA, linear discriminant analysis; QDA, quadratic discriminant analysis; MLPNN with BP, multilayer perceptron neural network with the back propagation training algorithm; RBF, radial basis function; SEN, sensitivity; SPE, specificity; SVM, support vector machine.

TABLE 2 Performance of the proposed method with Sym 3 using the HMM classifier based on all seven classes of BNDB

Class	SEN (%)	SPE (%)	ACC (%)
Z-S	100.00	100.00	100.00
O-S	100.00	100.00	100.00
N-S	99.90	100.00	100.00
F-S	99.85	99.01	99.77
ZO-S	100.00	100.00	99.97
NF-S	98.85	99.12	98.95
ZONF-S	99.51	98.60	99.54
Total	**99.73 (0.43)**	**99.53 (0.60)**	**99.78 (0.40)**

Note: Numbers in parentheses indicate standard deviations. 'BNDB' is omitted from the class names. Bold values indicate the average performances of all seven classes of BNDB.
Abbreviations: ACC, accuracy; SEN, sensitivity; SPE, specificity.

LDA and QDA classifiers, the accuracy results were below 95% for both the IHDB and BNDB databases. Thus, the proposed ASCOT method achieved a robust performance with seven different classes, yielding accuracies of 95.90% (IHDB) and 97.20% (BNDB).

Table 2 shows the performance of the proposed method with seven classes using the HMM classifier (best performance) in BNDB. For the purpose of this study, the proposed method yielded satisfactory performances for all seven classes used for the classification of seizure waveforms of EEG signals. With the subset BNDB-S (seizure) corresponding to one subset (BNDB-Z-S, BNDB-O-S, BNDB-N-S, or BNDB-F-S), the proposed method yielded an average accuracy of 99.94%. Furthermore, the accuracy for ZONF-S, which included four subsets, was 99.54%.

4.3 | Performance comparison for various types of wavelet function

The decomposition of frequency bands was performed using the mother wavelet function that was most similar to the epileptic seizure waveform. In preprocessing, we already determined the suitable mother wavelet through confirming the cross-correlations between the epileptic seizure waveform and various mother wavelet functions. Thus, we assessed the performance by varying the mother wavelet functions.

As shown in Figure 6, using the proposed method with Sym of order 3, the highest accuracies of 97.45% and 99.75%, respectively, were obtained for IHDB and BNDB. Meanwhile, the lowest accuracy results for IHDB and BNDB were 76.15% and 70.88%, where *Db* of order 8 was utilized.

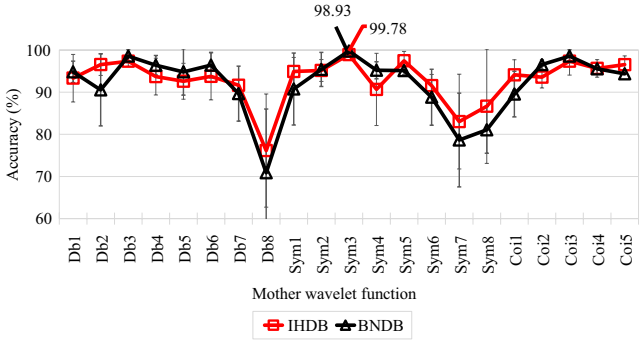

FIGURE 6 Performance of the proposed method using various types of mother wavelet function based on the HMM classifier

4.4 | Performance comparison using various window sizes

In this section, we evaluate the performance of the proposed ASCOT method by varying the window sizes to assess its sensitivity. It is important to determine optimal and shorter window sizes, owing to the requirements of prediction and detection of epileptic seizures in advance or a real-time system, and long-term monitoring for interpretation. We set various window sizes (segment lengths) of 50, 250, 1000, and 4000, and compared the average accuracies when the ASCOT feature extraction method with HMM was employed.

As shown in Figure 7, for IHDB the result was 98.93% when the length was 4000, which was approximately 7.88% higher than the result with the window length of 50. Further, for BNDB the proposed method with a window size of 4000 yielded the best performance (SEN: 99.73%, SPE: 99.53%; ACC: 99.78). Conversely, when a window size of 50 was adopted the performance was the worst (SEN: 96.62%, SPE: 91.28%; ACC: 94.46%), as shown in Figure 8. This is because the amount of training and testing data (input) for classification decreases as the window size becomes smaller. However, our method yielded robust performances of over approximately 90% for both databases when the shortest window size of 50 was used.

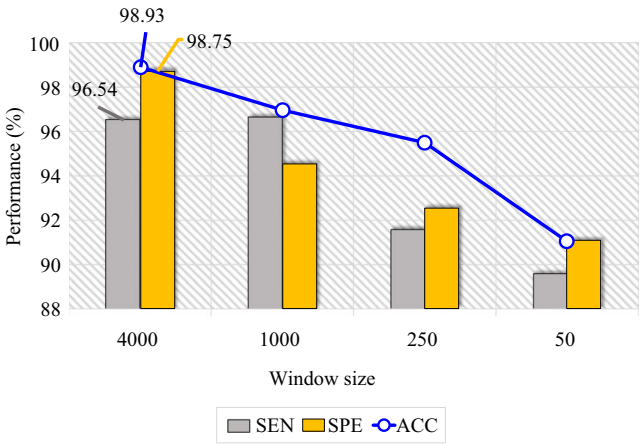

FIGURE 7 Performance of the proposed method using various window sizes based on IHDB

5 | DISCUSSION

In this paper, we propose the novel ASCOT method for the detection of epileptic seizure waveforms in EEG signals. Its reliable performance in our database and a public database demonstrate that the proposed method achieves robust seizure detection. However, some issues still remain to be discussed, such as the threshold generation step. In addition, we will discuss the performance of the proposed method comparatively for the two databases.

5.1 | Threshold generation

In the feature extraction step, we have already generated various thresholds to count wavelet coefficients to measure the frequency. Although our approach is based on the zero-crossing method [21–24], we used various thresholds according to the level t (refer to the Section 3.2. Feature extraction) for repetitive calculations. Here, we need to find a suitable optimized threshold, because we generate thresholds based on the maximum value of the coefficients of each subband. We are still investigating how to optimize the threshold. However, the main advantage of our method is that it can easily obtain frequency information in the time domain using the rate of change of the counted values, and it is possible to effectively reflect the inherent characteristics of seizure waveforms. Therefore, we obtained the counted values of the coefficients according to time-varying levels, and then utilized the rate of change of these values.

5.2 | Comparison with other approaches in BNDB

BNDB includes seizure, nonseizure, and normal EEG signals, and we utilized this database for the validation of our method. Other studies that have validated their algorithms using BNDB are summarized in Table 3 [10,14,15,34–43]. Sharma et al [10] proposed the time-frequency flexible wavelet transform and fractal dimension, and the performance of their method was only approximately 0.03% higher than that of our method in the classification between ZO and S classes. However, their overall average performance was 99.34% (ZS, OS, NS, FS, ZO-S, NF-S, and ZONF-S), which is slightly lower than that of our method (approximately 0.42%). Toward et al [14] utilized key-points based on local binary patterns (LBP) with SVM, and they validated the performance of ZO-S, NF-S, and ZONF. The average performance was higher than that of our method, but the difference is only 0.1%. The results obtained using the methods proposed by Bhattacharyya et al [15], Sharma et al [34], Peker et al [36], and Samiee et al [37] were slightly worse or nearly equivalent to those of our proposed method. In addition, although robust performances were obtained in [38–41] based on LBP, which has an advantage in terms of calculation efficiency, these were inferior to the performance using our method. Recently, various methods based on PCA have been introduced and utilized for epileptic seizure detection in EEG signal processing [42,43]. Jaiswal et al [42] proposed a seizure detection method based on the global modular PCA (GModPCA), which has the advantage of both local and global variations. Further, Jaiswal et al [43] introduced two effective approaches to epileptic seizure detection methods using subpattern-based PCA (SpPCA) and cross-subpattern correlation-based PCA (SubXPCA). Both of these have effective time and space complexities, which also play an important role in evaluating the effectiveness in real-time applications. On comparing the various PCA methods with our method, it is found that the detection performances of the methods based on PCA are equivalent with or are slightly inferior to our method. Meanwhile, the result of the method proposed by Sharma et al [35] was better than our result pertaining to the classification between NF and S. However, it is difficult to precisely compare the performances, because the results of other datasets could not be represented. Although

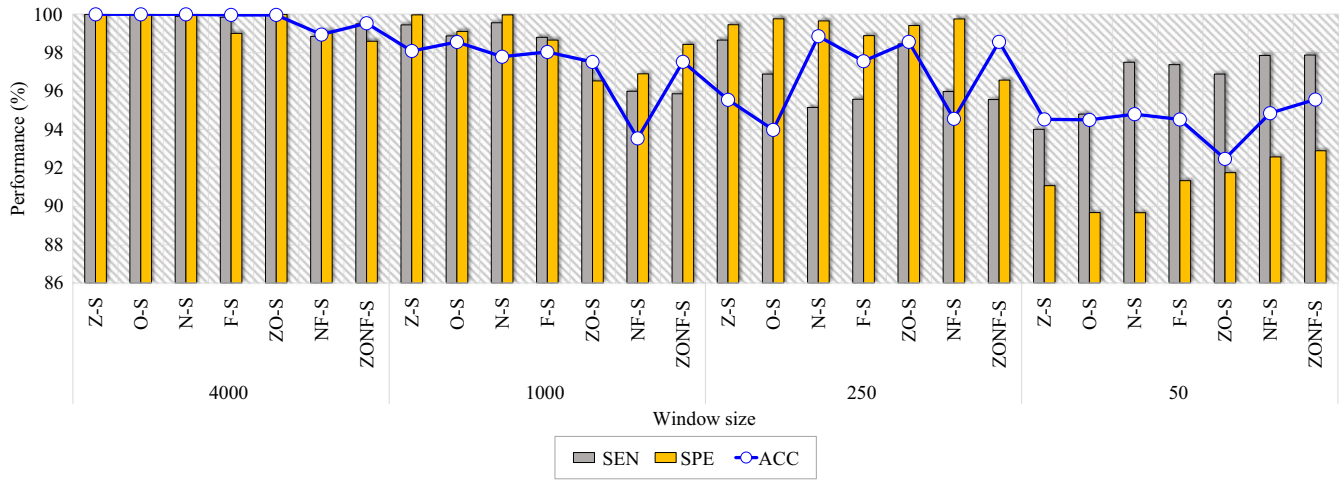

FIGURE 8 Performance of the proposed method using various window sizes based on BNDB

TABLE 3 Performance comparison with previous studies on seizure detection based on BNDB

Publication	Method	Class	ACC (%)
Sharma et al [10]	Time-frequency flexible wavelet transform and fractal dimension	Z-S O-S N-S F-S ZO-S NF-S ZONF-S	100.00 100.00 99.00 98.50 100.00 98.67 99.20
Tiwari et al [14]	Key-point based on local binary pattern + SVM with radial basis function (RBF)	ZO-S NF-S ZONF-S	100.00 99.45 99.31
Bhattacharyya et al [15]	TQWT-based multi-scale K-NN entropy	Z-S O-S N-S F-S ZONF-S	100.00 100.00 99.50 98.00 99.00
Sharma et al [34]	Phase space representation of intrinsic mode functions	NF-S	98.67
Sharma et al [35]	Improved eigenvalue decomposition of Hankel matrix and Hilbert transform with LS-SVM classifier	NF-S	100.00
Peker et al [36]	Dual tree complex wavelet transform and complex valued neural network	Z-S ZONF-S ZO-FN-S	100.00 99.15 98.28
Samiee et al [37]	Rational discrete SFTF and MLP classifier	Z-S O-S N-S F-S ZONF-S	99.80 99.30 98.50 94.90 98.10
Kumar et al [38]	[1)]1D-Local binary pattern [2)]Multi-level local patterns	NF-S	97.67[1)] 98.67[2)]
Kaya et al [39]	[3)]Local binary pattern (all pattern) with BayesNet [4)]Local binary pattern (uniform pattern) with BayesNet	[3)]Z-S [4)]N-S [3)]Z-N-S	99.50 95.50 95.67
Kumar et al [40]	Local binary pattern with nearest neighbor classifier	NF-S	98.33
Jaiswal et al [41]	[5)]Local Neighbor Descriptive Pattern with Artificial neural network [6)]1D-Local gradient pattern with Artificial neural network	Z-S O-S N-S F-S NF-S ZONF-S	99.82[5)] 99.80[6)] 99.25[5)] 98.92[6)] 99.10[5)] 99.02[6)] 99.07[5)] 98.18[6)] 98.88[5)] 98.78[6)] 98.72[5)] 98.65[6)]
Jaiswal et al [42]	CModPCA and SVM	Z-S O-S N-S F-S ZO-S NF-S ZONF-S	100.00 99.20 98.50 94.20 99.66 95.80 97.17
Jaiswal et al [43]	[7)]SpPCA and SVM [8)]SubXPCA and SVM	[7)]Z-S [7)]O-S [7)]N-S [7)]F-S [7)]ZO-S [7)]NF-S [7)]ZONF-S [8)]Z-S [8)]O-S [8)]N-S [8)]F-S [8)]ZO-S [8)]NF-S [8)]ZONF-S	100.00 99.50 99.50 95.50 99.66 96.66 97.60 100.00 99.50 99.50 95.50 99.66 96.66 97.40
This study	**Adaptive slope of wavelet coefficient counts over various thresholds based on HMM**	**Z-S** **O-S** **N-S** **F-S** **ZO-S** **NF-S** **ZONF-S**	**100.00** **100.00** **100.00** **99.77** **99.97** **98.95** **99.54**

Bold values indicate the result of the proposed method in this study. Each superscript number represents the accuracy of the method used.

Sharma et al utilized different datasets extracted from BNDB, we verified that our method is robust and reliable in BNDB in terms of the average accuracy (ACC) through its performance results. It should be noted that the classification performances of our method for both BNDB-N-S and BNDB-F-S were more robust than those of other methods. Through these comparisons, although our algorithm was not intended to detect interictal waveforms, we could achieve promising results in interictal waveforms of EEGs.

5.3 | Performance comparison with other approaches using various window sizes

To evaluate the effect of the window size, we employed various window sizes of 4000, 1000, 250, and 50, which were also used in [14,34,37]. As shown in Figure 7, the performance rapidly degraded as the window size was reduced to 50 for BNDB. However, our method achieved a relatively high performance of 97.09% as the overall average for the four window sizes. Similar results were generally observed for IHDB, as shown in Figure 8, and the performance was strong for all four window sizes, with an average of 95.62%. In real-time systems, seizure detection methods require less data (a smaller window size) to detect the sudden occurrence of a seizure. Therefore, we verified that the proposed ASCOT feature extraction method can suitably detect the occurrence of a seizure with a small amount of data.

Previous studies that have validated their algorithms using various window sizes are summarized in Table 4. Samiee et al [37] yielded the best performance of 98.3% when the window size was 512. However, that study used classes from different datasets from BNDB than we considered. Sharma et al [34] yielded satisfactory performances with window sizes of 1000, 250, and 50 for BNDB. The authors only utilized four types of dataset, whereas we used seven. Tiwari et al [14] verified the performance of their method using the Hospital of New Delhi [44] database along with BNDB. Compared to the methods mentioned above, our method achieved a robust performance for seizure detection with a small window size. Thus, we can conclude that the ASCOT method is suitable for application in a real-time system to detect momentary seizures and detect seizure waveforms in long-term monitoring for effective interpretation.

5.4 | Processing time

Long-term EEG monitoring for seizure detection requires not only a high accuracy but also a fast feature extraction time, as a considerable amount of data is recorded over 24 hours. Furthermore, the feature extraction techniques for real-life monitoring should be computationally efficient. The average times required for feature extraction from datasets with 50, 250, 1000, and 4000 points were computed using the proposed ASCOT method. The experiment was performed on an Intel ® core i5-6600 CPU (3.30 GHz) with 4 GB RAM. When the number of data points in the dataset were 50, 250, 1000, and 4000, the calculation times were approximately 0.25, 0.5, 5, and 20 seconds, respectively. Feature extraction for the proposed method took 0.0031, 0.0057, 0.0226, and 0.1124 seconds, respectively.

In previous studies, the key point-based LBP method [14], SP LBC with an artificial neural network (ANN) [45], SP LGC with ANN [45], and SP LNDB with ANN [45] had execution times of 3.51, 0.1092, 0.1123, and 0.1571 seconds, respectively, for 4092 data points. Furthermore, the execution times of LNDP with ANN [41], 1D-LGP with ANN [41], and 1D-LBP with BayesNet [41] were 0.048, 0.082, and 0.1305 seconds, respectively. In [46], the authors employed a fuzzy method, and FCRE-ELM and FCRE-SVM

TABLE 4 Performance comparison with previous studies for seizure detection using various window sizes based on BNDB

Publication	Sampling Rate (Hz)	Database	Window size (sample)	ACC (%)
Samiee et al [37]	173.61	Bonn University	1024	97.60
			512	98.30
			256	97.80
			173	96.20
Tiwari et al [14]	173.61	Hospital of New Delhi [40]	519	99.89
			400	99.07
			300	97.67
			200	94.15
			100	88.50
	173.00	Bonn University	4000	98.67
			2000	97.00
			1000	96.00
			500	94.33
Sharma et al [34]	173.61	Bonn University	4000	99.39
			1000	98.03
			250	97.15
			50	92.32
This study	**173.61**	**Bonn University**	**4000**	**99.78**
			1000	**97.30**
			250	**96.66**
			50	**94.46**
	200.00	**Inha University Hospital**	**4000**	**98.93**
			1000	**96.98**
			250	**95.51**
			50	**91.05**

Bold values indicate the result of the proposed method in this study.

required 0.065 and 0.2425 seconds for processing, respectively. Although the processing time of DWT-SVM [47] was not specified, its classification time was 0.2998 second. Finally, LS-SVM based on the wavelet transform has a processing time of 0.014 second (2 seconds dataset) for feature extraction [10]. Comparing these results for the feature extraction processing time, we conclude that the proposed ASCOT method is suitable for application to real-time systems and for interpreting long-term EEG monitoring.

6 | CONCLUSION

This study proposes a novel feature extraction algorithm for seizure detection, to overcome the limitations of long-term EEG monitoring. The proposed method utilizes coefficients from the discrete wavelet transform, and calculates the adaptive slope of coefficients counts over various thresholds. The main advantage of this approach is that it enhances the detection performance by applying a suitable mother wavelet function (*Symlet* of order 3) for the discrete wavelet transform, and can measure the frequency of an EEG signal with a short window size. We validated our method using our own database and a public database.

The proposed method achieved a reliable performance on the two databases BNDB (SEN: 99.73%, SPE: 99.53%, and ACC: 99.78%) and IHDB (SEN: 96.54%, SPE: 98.75%, and ACC: 98.93%). Furthermore, the total average results for the proposed method with window sizes of 4000, 1000, 250, and 50, were 97.05% (BNDB) and 95.62% (IHDB). In future work, we will improve our method in terms of the threshold generation step, and apply it to automated seizure detection for online (in real-time) and long-term EEG monitoring.

ACKNOWLEDGMENTS

This research was supported in part by the Basic Science Research Program through the National Research Foundation of Korea funded by the Ministry of Education (2018R1D1A1B07042602), and in part by the Industrial Technology Innovation Program funded by the Ministry of Trade, Industry & Energy (MI, Korea) [10073154, Development of human-friendly human–robot interaction technologies using human internal emotional states], and in part by the Institute for Information and Communications Technology Promotion (IITP) grant funded by the Korea government (MSIT) (No. 2019-0-00064, Intelligent Mobile Edge Cloud Solution for Connected Car).

CONFLICT OF INTEREST

None declared.

ORCID

Miran Lee https://orcid.org/0000-0003-4851-5030
Deok-Hwan Kim https://orcid.org/0000-0002-6048-9392

REFERENCES

1. F. Mormann et al., *Seizure prediction: the long and winding road*, Brain **130** (2006), no. 2, 314–333.
2. B. Litt and K. Lehnertz, *Seizure prediction and the preseizure period*, Curr. Opin. Neurol. **14** (2002), no. 2. 173–177.
3. V. Joshi, R. B. Pachori, and A. Vijesh, *Classification of ictal and seizure-free EEG signals using fractional linear prediction*, Biomed. Signal Process. Contr. **9** (2013), 1–5.
4. L. Guo et al., *Automatic epileptic seizure detection in EEGs based on line length feature and artificial neural networks*, J. Neurosci. Methods **191** (2010), no. 1, 101–109.
5. A. Subasi and M. I. Gursoy, *EEG signal classification using PCA, ICA, LDA and support vector machines*, Expert Syst. Applicat. **37** (2010), no. 12, 8659–8666.
6. S. Xie et al., *Feature extraction via dynamic PCA for epilepsy diagnosis and epileptic seizure detection*, in Proc. IEEE Int. Work. Machine Lear. Signal Process., Kittila, Finland, 2010, pp. 337–342.
7. S. Ghosh-Dastidar, H. Adeli, and N. Daddmehr, *Principal component analysis-enhanced cosine radial basis function neural network for robust epilepsy and seizure detection*, IEEE Trans. Biomed. Eng. **55** (2008), no. 2, 512–518.
8. J. Kevric and A. Subasi, *The effect of multiscale PCA de-noising in epileptic seizure detection*, J. Med. Syst. **38** (2014), no. 10, 131–143.
9. Y. Kumar, M. L. Dewal, and R. S. Anand, *Epileptic seizures detection in EEG using DWT-based ApEn and artificial neural network*, Signal Image Video Process **8** (2012), no. 7, 1323–1334.
10. M. Sharmar, R. B. Pachori, and U. R. Acharya, *A new approach to characterize epileptic seizures using analytic time-frequency flexible wavelet transform and fractal dimension*, Pattern Recogn. Lett. **94** (2017), 172–179.
11. D. Bhati, R. B. Pachori, and V. M. Gadre, *Time-frequency localized three-band biorthogonal wavelet filter bank using semidefinite relaxation and nonlinear least squares with epileptic seizure EEG signal classification*, Digit. Signal Process. **62** (2017), 259–273.
12. H. Ocak, *Automatic detection of epileptic seizures in EEG using discrete wavelet transform and approximate entropy*, Expert Syst. Applicat. **36** (2009), no. 2, 2027–2036.
13. S. Nasehi and H. Pourghassem, *Automatic prediction of epileptic seizure using kernel fisher discriminant classifiers*, in Proc. Int. Compt. Bio-Med. Instrum., Wuhan, China, 2011, pp. 200–203.
14. A. K. Tiwari et al., *Automated diagnosis of epilepsy using key-points based local binary pattern of EEG signals*, IEEE J. Biomed. Health. **21** (2017), no. 4, 888–896.
15. A. Bhattacharyya et al., *Tunable-Q wavelet transform based multiscale entropy measure for automated classification of epileptic EEG signals*, Appl. Sci. **7** (2017), no. 4, 385–402.
16. R. B. Pachori and S. Patidar, *Epileptic seizure classification in EEG signals using second-order difference plot of intrinsic mode functions*, Comput. Methods Programs Biomed. **113** (2014), no. 2, 494–502.

17. V. Bajaj and R. B. Pachori, *Epileptic seizure detection based on the instantaneous area of analytic intrinsic mode functions of EEG signals*, Biomed. Eng. Lett. **3** (2013), no. 1, 17–21.
18. V. Bajaj and R. B. Pachori, *Classification of seizure and nonseizure EEG signals using empirical mode decomposition*, IEEE Trans. Inf. Technol. Biomed. **16** (2012), no. 6, 1135–1142.
19. R. B. Pachori and V. Bajaj, *Analysis of normal and epileptic seizure EEG signals using empirical mode decomposition*, Comput. Methods Programs Biomed. **104** (2011), no. 3, 373–381.
20. R. B. Pachori, *Discrimination between ictal and seizure-free EEG signals using empirical mode decomposition*, Res. Lett. Signal Process. **2008** (2008), no. 14, 1–5.
21. I. Conradsen et al., *Automated algorithm for generalised tonic-clonic epileptic seizure onset detection based on sEMG zero-crossing rate*, IEEE Trans. Biomed. Eng. **59** (2012), no. 2, 579–585.
22. S. Elgohary, S. Eldawlathly, and M. I. Khalil, *Epileptic seizure prediction using zero-crossings analysis of EEG wavelet detail coefficients*, in Proc. IEEE Conf. Comput. Intell. Bioinformatics. Comput. Biol., Chiang, Thailand, Oct. 2016, pp. 1–6.
23. A. S. Zandi et al., *Predicting epileptic seizures in scalp EEG based on a variational bayesian faussian mixture model of zero-crossing intervals*, IEEE Trans. Biomed. Eng. **60** (2013), no. 5, 1401–1413.
24. A. S. Zandi et al., *Predicting temporal lobe epileptic seizures based on zero–crossing interval analysis in scalp EEG*, in Proc. Ann. Int. Conf. Eng. Medi. Biol. Soc., Buenos Aires, Argentina, 2010, pp. 5537–5540.
25. A. Subasi, *Application of adaptive neuro-fuzzy inference system for epileptic seizure detection using wavelet feature extraction*, Comput. Biol. Med. **37** (2007), no. 2, 227–244.
26. M. R. Lee et al., *Classification of both seizure and non-seizure based on EEG signals using hidden markov model*, in Proc. Int. Conf. BIGCOMP., Shanghai, China, 2018, pp. 469–474.
27. R. Oostenveld and P. Praamstra, *The five percent electrode system for high-resolution EEG and ERP measurements*, Clin. Neurophysiol. **112** (2001), no. 4, 713–719.
28. M. R. Lee et al., *A novel R peak detection method for mobile environments*, IEEE Access **6** (2018), 51227–51237.
29. R. G. Andrzejak et al., *Indications of nonlinear deterministic and finite dimensional structures in time series of brain electrical activity: dependence on recording region and brain state*, Phys. Rev. E. **64** (2001), no. 6, 061907:1–8.
30. K. P. Indiradevi et al., *A multi-level wavelet approach for automatic detection of epileptic spikes in the electroencephalogram*, Comput. Biol. Med. **38** (2008), no. 7, 805–816.
31. R. W. Wall, *Simple methods for detecting zero crossing*, in Proc. Ann. Conf. Industrial Elect. Soc., Roanoke, VA, USA, 2004, pp. 2477–2481.
32. M. Z. Uddin, D. H. Kim, and T. S. Kim, *A human activity recognition system using HMMs with GDA on enhanced independent component features*, Int. Arab J. Inf. Technol. **12** (2015), no. 3, 304–310.
33. M. H. Abdullah, J. M. Abullah, and M. Z. Abdullah, *Seizure detection by means of hidden Markov model and stationary wavelet transform of electroencephalograph signals*, in Proc. Biomed. Health Informatics, Hong Kong, China, 2012, pp. 62–65.
34. R. Sharma and R. B. Pachori, *Classification of epileptic seizures in EEG signals based on phase space representation of intrinsic mode functions*, Expert Syst. Applicat. **42** (2015), no. 3, 1106–1117.
35. R. R. Sharma and R. B. Pachori, *Time-frequency representation using IEVDHM-HT with application to classification of epileptic EEG signals*, IET Sci. Meas. Technol. **12** (2017), no. 1, 72–82.
36. M. Peker, B. Sen, and D. Delen, *A novel method for automated diagnosis of epilepsy using complex-valued classifiers*, IEEE J. Biomed. Health Inform. **20** (2015), no. 1, 108–118.
37. K. Samiee, P. Kovacs, and M. Gabboouj, *Epileptic seizure classification of EEG time-series using rational discrete short-time Fourier transform*, IEEE Trans. Biomed. Eng. **62** (2014), no. 2, 541–552.
38. T. S. Kumar, *Classification of seizure and seizure-free EEG signals using local binary patterns*, Biomed. Signal Process. Contr. **15** (2015), 33–40.
39. Y. Kaya et al., *1D-local binary pattern based feature extraction for classification of epileptic EEG signals*, Appl. Math. Comput. **243** (2014), 209–219.
40. T. S. Kumar et al., *Classification of seizure and seizure-free EEG signals using multi-level local patterns*, in Proc. Int. Conf. Digit. Signal Process., Hong Kong, China, Aug. 2014, pp. 646–650.
41. A. K. Jaiswal and H. Banka, *Local pattern transformation based feature extraction techniques for classification of epileptic EEG signals*, Biomed. Signal Process. Contr. **34** (2017), 81–92.
42. A. K. Jaiswal and H. Banka, *Epileptic seizure detection in EEG signal with GModPCA and support vector machine*, Biomed. Mater. Eng. **28** (2017), no. 2, 141–157.
43. A. K. Jaiswal and H. Banka, *Epileptic seizure detection in EEG signal using machine learning techniques*, Australas. Phys. Eng. Sci. Med. **41** (2018), no. 1, 81–94.
44. T. Gandhi et al., *Expert model for detection of epileptic activity in EEG signature*, Expert Syst. Appl. **37** (2010), no. 4, 3513–3520.
45. N. J. Sairamya et al., *Detection of epileptic EEG signal using improved local pattern transformation methods*, Circ. Syst. Signal Process. **37** (2018), no. 12, 1–22.
46. J. L. Song and R. Zhang, *Automatic seizure detection using a novel EEG feature based on nonlinear complexity*, in Proc. Int. Joint Conf. Neural Netw., Vancouver, Canada, 2016, pp. 1686–1695.
47. Y. Kumar, M. L. Dewal, and R. S. Anand, *Epileptic seizure detection using DWT based fuzzy approximate entropy and support vector machine*, Neurocomput. **133** (2014), 271–279.

AUTHOR BIOGRAPHIES

Miran Lee received an MS degree in Electronics Engineering from Inha University. From 2016 to 2018, she worked with the Center for Bionics, Korea Institute of Science and Technology (KIST), Seoul, South Korea. She is a PhD student of Information Science and Engineering at Ritsumeikan University, Shiga, Japan. Her research interests include biomedical interface, pattern recognition, bio-signal processing (EMG, EEG, EMG, and ECG), human-interaction robot design and control, and bio-inspired systems.

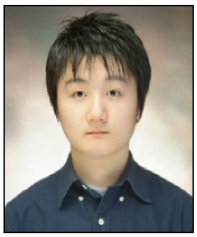

Jaehwan Ryu received MS and PhD degrees in Electronics Engineering from Inha University. He is a research engineer at Sammi Information System, Seoul, Rep. of Korea. His research interests include bioengineering, embedded systems, signal processing, hyperspectral imaging, geographic information systems, and bio-inspired systems.

Deok-Hwan Kim received MS and PhD degrees in Computer Engineering from the Korea Advanced Institute of Science and Technology. He is a professor in the School of Electronics Engineering at Inha University, Incheon, Rep. of Korea. His research interests include embedded systems, storage systems, multimedia systems, and bio-inspired systems.